

1  
2 **Technical Note: On HALOE stratospheric water vapor variations and trends at Boulder,**  
3 **Colorado**

4 **by**

5 **Ellis Remsberg**

6 **Science Directorate**

7 **21 Langley Blvd., Mail Stop 401B**

8 **NASA Langley Research Center**

9 **Hampton, Virginia USA, 23681**

10 (email: [Ellis.E.Remsberg@nasa.gov](mailto:Ellis.E.Remsberg@nasa.gov))

11 **Atmospheric Chemistry and Physics Journal**

12 **(~~March~~June 2023)**

13 **Abstract.** This study compares time series of stratospheric water vapor (SWV) data at 30 hPa  
14 and 50 hPa from 1993 to 2005, based on sets of Halogen Occultation Experiment (HALOE)  
15 profiles above the Boulder, CO (40°N, 255°E) region and on local frost-point hygrometer (FPH)  
16 measurements. Their differing trends herein agree with most of the previously published  
17 findings. ~~The~~ FPH trends are presumed to be accurate within their data uncertainties, and there  
18 are no known measurement biases affecting the HALOE trends. However, the seasonal  
19 sampling from HALOE is deficient at 40°N from 2001 to 2005, especially during late winter and  
20 springtime. HALOE time series at 20 hPa clearly show a springtime maximum in SWV at 40°N.  
21 ~~The retrievals of HALOE SWV have significant corrections for interfering aerosol extinction~~  
22 ~~following the eruption of Pinatubo, but there is no evidence that those corrections cause incorrect~~  
23 ~~SWV trends after 1992. Accordingly, this~~ This study finds that the SWV trends from HALOE  
24 and FPH nearly agree within ~~their~~ uncertainties at 30 hPa, but not at 50 hPa, for the more limited  
25 time span of 1993 to 2002. ~~HALOE SWV have significant and uncertain corrections for~~  
26 ~~interfering aerosol extinction after 1992 at 50 hPa, but not at 30 hPa.~~ Northern hemisphere time  
27 series and daily plots of SWV from the Limb Infrared Monitor of the Stratosphere (LIMS)  
28 experiment indicate that there is transport of filaments of high SWV from polar to middle  
29 latitudes during dynamically active, winter and springtime periods. Although FPH  
30 measurements sense SWV variations at all scales, the HALOE time series do not resolve  
31 ~~small~~ smaller-scale ~~structure~~ structures because its time series data are based on an average of four

32 or more occultations within a finite latitude/longitude sector. It is concluded that the variations  
33 and trends of HALOE SWV are ~~accurate for~~reasonable at 40°N and 30 hPa from 1993 to 2002 at  
34 ~~40°N~~ and in accord with the spatial scales of its measurements and ~~its~~ sampling ~~frequency over~~  
35 ~~time~~frequencies.

36

## 37 1. Background and Objective

38 There have been numerous studies of long-term changes of stratospheric water vapor (SWV)  
39 mixing ratios (e.g., Konopka, et al., 2022; Hegglin et al., 2014; Hurst et al., 2011). SWV trends  
40 in the lowermost stratosphere are affected mainly by non-zonal variations of the cold-point  
41 temperature (CPT) at the tropical tropopause, followed by transport of the associated relatively  
42 dry, entry-level air. Hegglin et al. (2014) also report on the roles of the oxidation of methane to  
43 water vapor in the middle and upper stratosphere and of changes in the Brewer/Dobson  
44 circulation (BDC) on water vapor trends throughout the stratosphere. One remaining puzzle is  
45 that the SWV trends from frost-point hygrometer (FPH) measurements above Boulder, CO, are  
46 more positive (or less negative) than zonal average and Boulder region analyses of SWV from  
47 the Halogen Occultation Experiment (HALOE), ~~and those differences increase with altitude~~  
48 (Scherer et al., 2008). Lossow et al. (2018) reported that those differences increase with altitude,  
49 and they cautioned that ~~the~~ trends over Boulder may not be representative of zonal-mean values,  
50 ~~and some years~~. Konopka et al. (2022) found from reanalysis data that there is a moistening  
51 above the Boulder region during late boreal winter and spring.

52

53 The present study reconsiders in Section 2 the HALOE SWV trends and variations ~~at 30 hPa~~  
54 ~~from HALOE measurements~~ near Boulder for 1993 through 2005 and compares them in Section  
55 3 with those from the Boulder FPH measurements that are assumed to be accurate. ~~Section 4~~  
56 ~~considers whether there is any bias for the HALOE SWV trends and whether there is evidence~~  
57 ~~for a springtime moistening at 40°N. The focus is on the trend differences at 30 hPa, where~~  
58 Lossow et al. (2018) found that they were largest. Section 4 reports on the SWV trend  
59 differences for the same years at 50 hPa, or where there may be biases in HALOE SWV from its  
60 corrections for interfering aerosols. Section 5 shows a time series of northern hemisphere SWV  
61 near 30 hPa from the Nimbus 7 Limb Infrared Monitor of the Stratosphere (LIMS) dataset of

62 1978-1979, ~~as a diagnostic for a source of elevated SWV during springtime.~~ Daily plots of  
63 LIMS geopotential height (GPH) and SWV show the effects of meridional transport of SWV to  
64 40°N during a dynamically active period of February 1979. That example provides evidence  
65 of a late winter to spring moistening in the Boulder region. There are also instances of elevated  
66 SWV in the HALOE SWV-time series of at subpolar latitudes at that time of year. Section 6  
67 concludes that the HALOE SWV variations and trends at 40°N are understandable ~~and~~  
68 ~~agree~~compared with those from FPH, given the spatial scales of their measurements ~~and~~ the  
69 reduction in sampling by HALOE after 2001, and possible HALOE SWV biases from interfering  
70 aerosols.

71

## 72 2. Time series analyses of HALOE SWV near Boulder

73 SWV time series from the HALOE dataset are analyzed by multiple linear regression (MLR)  
74 techniques in the manner of Remsberg (2008) and Remsberg et al. (2018a). ~~Figure 1 shows~~  
75 ~~HALOE time series data from late 1991 through 2005 for the Boulder sector plus an MLR model~~  
76 ~~fit to them, after correction for autoregressive effects having a lag-1 coefficient (AR1) of 0.35.~~  
77 Although HALOE began operations in October 1991, its SWV profiles are degraded in the lower  
78 stratosphere in 1991 through mid-1992 because of solar tracking anomalies in the presence of the  
79 very large extinction effects from Pinatubo aerosols. ~~The MLR modeling of the data in Fig. 1~~  
80 ~~extends from January 1993 onward. Yet, there are indications that HALOE SWV is larger for~~  
81 ~~SR than for SS from 2002 through 2005. Those apparent differences are because HALOE was~~  
82 ~~turned on later following a UARS yaw maneuver and turned off a bit earlier prior to the next yaw~~  
83 ~~event, to conserve power on the UARS spacecraft those years. That change in operating~~  
84 ~~procedure meant that there were few to no HALOE SR measurements near 40°N during late~~  
85 ~~winter and springtime after 2001. Figure 1a shows HALOE time series data from late 1991~~  
86 ~~through 2005 for the Boulder sector.~~

87

88 The Boulder region HALOE SWV points of Fig. 1a are for 30 hPa and are based on averages of  
89 profiles within the latitude range of  $40 \pm 4^\circ\text{N}$  and the longitude range of  $255 \pm 35^\circ\text{E}$ , since HALOE  
90 seldom measured profiles at the exact location of Boulder. A rather narrow latitude range was

91 chosen for this study because there is a significant latitudinal gradient in SWV near 40°N in both  
92 fall and springtime. The finite longitude range of  $\pm 35^\circ$  attains four or more profiles, ~~most times,~~  
93 from the SR or SS orbital crossings near Boulder, ~~most times,~~ and it is sufficient for ~~resolving~~  
94 ~~any~~ ~~indicating low~~ zonal ~~wave-1 and wave-2 features in wavenumber effects on~~ the SWV field.  
95 ~~The data in Fig. 1a from January 1993 onward are fit with an MLR model that corrects for~~  
96 ~~effects of lag-1 autoregression (AR1) and accounts for memory between adjacent data points~~  
97 ~~(Tiao et al., 1990); its AR1 coefficient is 0.35.~~ The MLR model fit to the data of January 1993  
98 through 2005 (~~solid curve~~) includes constant and linear trend terms plus periodic annual (AO),  
99 semiannual (SAO) and QBO-like terms, ~~where the~~. ~~The periodic~~ QBO-like term is  
100 approximated as a 28-mo cycle, ~~based on a Fourier analysis of an initial time series residual~~  
101 ~~after accounting for the seasonal terms.~~ The model also contains proxy terms for El  
102 Niño/Southern Oscillation (ENSO) ~~forcings~~ and solar cycle flux forcings. Significant terms are  
103 SAO, QBO-like, and ENSO proxy; the latter two terms account for differences from the fit of the  
104 HALOE data in Fig. ~~1a~~ versus that from a simple seasonal fitting, ~~as shown in SPARC (2000,~~  
105 ~~Chapter 3).~~ The ~~straight~~ ~~dashed~~ line in Fig. ~~1a~~ represents the sum of the constant term (4.84  
106 ppmv) and a linear trend ~~term~~ ~~coefficient~~ of  $-4.4 \pm 0.7(2\sigma) \% / 22 \pm 0.04$  ppmv/decade ~~with, having~~ a  
107 confidence interval (CI) of 95% ~~or a trend of~~  $-4.5 \pm 0.6(2\sigma) \% / \text{decade}$ . The SWV trend from  
108 Fig. ~~1a~~ agrees closely with ~~the zonal mean trend at 31.6 hPa previous trends~~ from HALOE  
109 ~~for data near 30 hPa in~~ the latitude range of 35°N to 45°N (Davis et al., 2016). ~~Figure 2 is the~~  
110 ~~residual (data minus MLR model curve) for the fit in Fig. 1, and its variations about the mean are~~  
111 ~~of order  $\pm 0.3$  ppmv;~~ ~~Lossow et al., 2018).~~

112  
113 ~~Occultation time series points for Fig. 1 are not spaced regularly, so the derived MLR terms are~~  
114 ~~non-orthogonal.~~ ~~However, the~~ ~~All~~ MLR term coefficients are reasonably accurate, if the seasonal  
115 sampling is good. ~~Otherwise, the analyzed errors for each term become~~ ~~Yet, there are~~  
116 ~~indications that HALOE SWV in Fig 1a is larger—~~ ~~for sunrise (SR) than for sunset (SS)~~  
117 ~~occultations from 2002 through 2005.~~ Those differences are because HALOE was turned on  
118 ~~later following a UARS yaw maneuver and turned off a bit earlier prior to the next yaw event, to~~  
119 ~~conserve power on the UARS spacecraft in late 2001.~~ ~~That change in operating procedure meant~~  
120 ~~that there were fewer HALOE SR measurements near 40°N during late winter and springtime~~

121 after 2001, although it remained good at lower latitudes (not shown). HALOE SWV for the  
122 longitude sector of Boulder but at the higher latitude zone of  $55\pm 10^\circ\text{N}$  is shown in Figure 1b,  
123 where the seasonal sampling is also better compared to that at  $40^\circ\text{N}$  in Fig. 1a. Note that  
124 HALOE SWV in Fig. 1b has rather high values in early 2002 or following stratospheric warming  
125 events in the winter of 2001-2002 (Charlton and Polvani, 2007). It may be that there was also  
126 transport of high SWV to  $40^\circ\text{N}$  at that time, but HALOE did not observe it directly.

127  
128 The negative HALOE SWV trend ~~is clearer in Fig. 1a~~ is affected by the downward shift in SWV  
129 values from 2002 onward, as noted by Randel et al. (2006), Scherer et al. (2008), Hegglin et al.  
130 (2014), and Konopka et al. (2022) noted that there was a clear according to the decrease in SWV  
131 in the tropical lower stratosphere in early 2001. They reported ~~on that there was~~ a delay in the  
132 decrease of SWV at  $40^\circ\text{N}$  because of the slow ascent of the dry tropical air plus the subsequent  
133 meridional transport and mixing of that air to middle latitudes. ~~As also noted by~~ Scherer et al.  
134 (2008) also noted that it is perhaps more appropriate to apply two, piecewise linear trend terms  
135 for the MLR modeling of the HALOE SWV data in Fig. ~~1a~~, where there is a break point in  
136 2002. ~~Instead~~ Thus, Figure ~~3-1c~~ shows a separate trend analysis of HALOE SWV for the Boulder  
137 sector at  $40^\circ\text{N}$ , but for 1993 to 2002; its average SWV value is 4.62 ppmv and its shorter trend  
138 term is no longer negative but positive at  $0.22\pm 0.04$  ppmv/decade (or  $+4.47\pm 0.87(2\sigma)$  %/decade-  
139 ). Finally, Figure 2 is the residual (data minus MLR model curve) for the fit in Fig. 1a, and its  
140 variations about the mean are of order  $\pm 0.3$  ppmv. An important test of the adequacy of the set  
141 of terms in its MLR model is whether any structure remains in the residual. No periodic  
142 structure is apparent in Fig. 2, even though there are clear seasonal gaps in the data series after  
143 2001.

### 144 145 **3. Time series of FPH measurements of SWV**

146 Figure ~~4-3a~~ is the SWV time series at 30 hPa from the FPH data at Boulder and for 1993-2005 for  
147 comparison with Fig. ~~1a~~. Individual FPH profiles were interpolated vertically to obtain SWV  
148 values at the 30-hPa level, and the FPH time series points are also spaced irregularly. SAO,  
149 QBO, ENSO, and Linear terms from the MLR model of Fig. ~~4-3a~~ have a significance ~~( $C$ )~~ of

150 better than 90%. The constant term is 4.70 ppmv, which is a bit less than that from the HALOE  
151 series (4.8384 ppmv) but within the estimated systematic uncertainties for both measurements.  
152 The FPH trend for 1993-2005 is positive or  $+0.17 \pm 0.07$  ppmv/decade (or  $+3.46 \pm 1.5$  ( $2\sigma$ )  
153 %/decade), as compared to the negative trend from HALOE ( $-4.45 \pm 0.76$  ( $2\sigma$ ) %/decade). There  
154 is also a change in trend around 2002 in the FPH data of Fig. 3a, although it is not so apparent  
155 because of the rather large scatter of the FPH points. Figure 53b shows the residual  
156 (corresponding FPH minus MLR) analysis for the time series data of Fig. 4, 1993 to 2002, which  
157 yields an average SWV of 4.62 ppmv and the FPH points exhibit more scatter compared agrees  
158 with the average HALOE residual in value from Fig. 21c. The larger scatter agrees reasonably  
159 with the upper limit, FPH uncertainty estimate of  $\pm 10\%$  or about  $\pm 0.5$  ppmv (SPARC, 2000).  
160 Accordingly, it is more difficult for FPH trend for 1993 to 2002 is  $+0.32 \pm 0.6$  ppmv/decade (or  
161  $+6.9 \pm 1.2$  %/decade), which is more positive than that of HALOE ( $+4.7 \pm 0.7$  %/decade) but only  
162 slightly outside the MLR modeling to resolve the periodic (SAO, AO, and QBO) variations from  
163 FPH data, while fitting a trend term overlapping envelope (e.g.,  $+5.7$  versus  $+5.4$  %/decade) from  
164 their mutual trend uncertainties.

165  
166 All data points of the FPH record are assumed to be valid and accurate to 10%, based on the  
167 extensive studies reported in Hurst et al. (2023). Yet, Fig. 4 shows that FPH has high SWV  
168 values of 5.8 ppmv on 22 May and 5.5 ppmv on 26 June 1996. Figure 4 shows the residual (FPH  
169 minus MLR) for the time series data of Fig. 3a, where the FPH points exhibit more scatter  
170 compared with the HALOE residual in Fig. 2. Data points of the FPH record are assumed to be  
171 valid and accurate to  $< 6\%$  or about  $\pm 0.3$  ppmv, according to the extensive studies of Hall et al.  
172 (2016). The rather large scatter in Fig. 4 exceeds that uncertainty. Local FPH measurements are  
173 sensitive to SWV variations across all spatial scales. Note that the structure in the FPH residual  
174 of Fig. 4 is aperiodic and presumably due to small-scale atmospheric variations in some  
175 instances. Accordingly, it is difficult for the MLR modeling to fit all the real structure in the  
176 FPH data, and its linear trend term is not highly significant. Conversely, each individual  
177 HALOE profile gives an SWV value that is an average across its tangent view path ( $\sim 300$  km)  
178 and with a vertical resolution of no better than two kilometers. The HALOE time series points

179 are also based on sector averages of four or more profiles. Thus, HALOE does not resolve SWV  
180 variations at small to intermediate scales.

181  
182 There are high FPH SWV values in Fig. 3 on 22 May (5.8 ppmv) and on 26 June 1996 (5.5  
183 ppmv), possibly due to elevated SWV in filaments of polar vortex air that were transported to  
184 and remained isolated above the location of Boulder for days to weeks (e.g., Manney et al. (  
185 2022)). A search of individual profiles from HALOE reveals SWV values of order 6.5 ppmv at  
186 60°N, 270°E in mid-March 1996. Temperature at that higher latitude location is only 200 K and  
187 methane is only 0.4 ppmv, both of which are characteristic of winter vortex air. HALOE also  
188 found a small region of high SWV (~5.8 ppmv) and low methane in several soundings near  
189 44°N, 170°E on 12 May 1996. In another instance, FPH has a value of 5.9 ppmv high SWV on  
190 12 April 2000. (5.9 ppmv). HALOE SWV approached 7.0 ppmv near 60°N, 270°E about a  
191 month earlier on 18 March 2000; there are also several values greater than 5.0 ppmv at 40°N on  
192 20 April 2000. Still, each individual HALOE profile gives SWV values that are an average  
193 across its tangent view path of order 300 km and with a vertical resolution of no better than two  
194 kilometers. The HALOE time series points are also based on sector averages of four or more  
195 profiles, so they do not resolve SWV variations at small to intermediate scales. Conversely, the  
196 local FPH measurements are sensitive to SWV variations across all spatial scales. HALOE values  
197 greater than 5.0 ppmv at 40°N on 20 April 2000. An example of a source of the elevated SWV  
198 is considered in Section 5.

199  
200 ~~There is also a change in trend around 2002 in the FPH data of Fig. 4, although it is not so~~  
201 ~~apparent because of the rather large scatter for the points of its data series. Figure 6 shows the~~  
202 ~~MLR analysis of FPH data for 1993 to 2002, which yields an average SWV of 4.64 ppmv that~~  
203 ~~agrees with the average value from HALOE in Fig. 3 (4.62 ppmv). The FPH trend for 1993 to~~  
204 ~~2002 is  $+5.8 \pm 1.2$  %/decade and agrees with that from HALOE ( $+4.4 \pm 0.8$  %/decade), at least~~  
205 ~~within their combined uncertainties.~~

206

#### 207 **4. Uncertainties for the HALOE SWV trends**

208 ~~As noted in the previous section, the SWV trend at 30 hPa from FPH is more positive (+5.8~~  
209 ~~%/decade) than that from HALOE (+4.4 %/decade) from 1993 to 2002, or prior to the episodic~~  
210 ~~decrease of SWV from 2001.~~ Gordley et al. (2009) reported that there are no indications of an  
211 instrument bias for the HALOE SWV trends. ~~However, HALOE SWV profiles may be affected~~  
212 ~~by residual effects from cloud tops and subvisible cirrus, as shown for HALOE ozone (Bhatt et~~  
213 ~~al., 1999).~~ As a result, the HALOE SWV trends at pressure levels of 100 hPa and even 70 hPa  
214 may not be accurate. ~~Harries et al. (1996) reported that a given HALOE~~  
215 ~~SWV profile is uncertain by 8% at 40 hPa because of interfering aerosols, and Hervig et al.~~  
216 ~~(1995) made significant~~ aerosol corrections for the retrieval of HALOE SWV ~~in the lower~~  
217 ~~stratosphere at 30 hPa and, especially at 50 hPa, following the Pinatubo eruption. Figure 5 is the~~  
218 ~~HALOE time series at 50 hPa; note that the abrupt decrease of SWV occurs in mid-2001. While~~  
219 ~~the HALOE trend is negative from 1993 to 2005, the MLR model fit is positive from December~~  
220 ~~1992 to mid-2001. Its SAO, AO, QBO, and ENSO terms are significant, its mean value is 4.28~~  
221 ~~ppmv, and its trend to mid-2001 is +3.7±1.4 %/decade.~~

222  
223 ~~Figure 6 is the~~ ~~Harries et al. (1996)~~ ~~estimated that a given HALOE SWV profile is uncertain by~~  
224 ~~6% to 8% at 10 hPa and 40 hPa, respectively, due to aerosols. Yet, the corrections are relatively~~  
225 ~~accurate with time because each individual SWV profile makes use of a corresponding estimate~~  
226 ~~of FPH time series at 50 hPa. It shows no clear change in 2001, largely a consequence of the~~  
227 ~~scatter in the data. Its mean value from late 1992 to mid-2001 is 4.21 ppmv, but its trend is~~  
228 ~~+10.8±1.7 %/decade or much larger than from HALOE. The HALOE versus FPH trend~~  
229 ~~difference at 50 hPa is qualitatively like that from Scherer et al. (2008, their Fig. 7). On the other~~  
230 ~~hand, at 30 hPa HALOE has lower aerosol extinction from another HALOE channel of the same~~  
231 ~~occultation sounding values and yields a SWV trend for 1993 to 2002 that agrees more nearly~~  
232 ~~with that of FPH (HALOE from Fig. 1c is +4.7 %/decade and FPH from Fig. 3b is +6.9~~  
233 ~~%/decade).~~

234  
235 ~~Corrections to SWV from interfering aerosols are more significant and extend for longer times at~~  
236 ~~50 hPa than at 30 hPa.~~ Aerosol extinction profiles are determined ~~for~~ ~~from~~ wavelengths of the  
237 HALOE gas filter correlation channels of HF, HCl, CH<sub>4</sub>, and NO (Hervig et al., 1995). Then,



238 corrections for the HALOE radiometer channels (H<sub>2</sub>O, NO<sub>2</sub>, and O<sub>3</sub>) are a modeled extrapolation  
239 ~~is with~~ wavelength from the NO channel aerosol profile at 5.26 micrometers. Example  
240 comparisons of retrieved HALOE SWV versus correlative measurements indicate that the  
241 modeled corrections are qualitatively ~~accurate~~ correct, even in 1992- (~~Hervig et al., 1996~~).  
242 Nevertheless, the model for aerosol absorption versus wavelength assumes a size distribution  
243 shape and an aqueous sulfuric acid composition (i.e., refractive index) that is constant with  
244 altitude and over time (~~Hervig et al., 1996~~). Effectively, the aerosol ~~correction~~  
245 ~~represents corrections represent~~ a change in aerosol number density only. That correction model  
246 ~~may not be very accurate~~ was employed for both a background aerosol layer, as well as for the  
247 decay of the Pinatubo aerosol layer, as it decays over time. Thus, there ~~may~~ can be a residual,  
248 time dependent bias for ~~the~~ HALOE SWV due to the aerosol correction model. Perhaps  
249 HALOE SWV is under corrected at 50 hPa for the effects of aerosols through the mid-1990s.

250  
251 HALOE SWV trends should be more accurate above the aerosol layer. As a check on that  
252 ~~possibility~~ likelihood, Figure 7 shows the corresponding fit of the HALOE SWV time series from  
253 1993 to 2002 at 40°N and 20 hPa, or just above the top of the volcanic aerosol layer. SWV has a  
254 positive vertical mixing ratio gradient with altitude, due to the oxidation of methane to SWV in  
255 the middle stratosphere, and average SWV at 20 hPa is 4.74 ppmv or a bit higher than that at 30  
256 hPa (4.62 ppmv). A combined AO/SAO maximum shows clearly in Fig. 7, where the AO  
257 amplitude is twice that of the SAO and the AO and SAO phase maxima are on 19 February and 9  
258 April, respectively. Those cycles confirm the late winter/early spring moistening found in  
259 reanalysis data at 40°N by Konopka et al. (2022).

260  
261 The HALOE SWV trend at 20 hPa for 1993-2002 is  $+6.69 \pm 0.9$  (2 $\sigma$ ) %/decade, which ~~is a bit~~  
262 ~~higher than agrees with~~ that at 30 hPa from FPH ( $+5.86.9 \pm 1.2$  %/decade) ~~at 30 hPa but within~~  
263 ~~uncertainties~~. (There are too few FPH data at 20 hPa for a direct trend comparison with  
264 HALOE.) ~~On the other hand~~ Yet, the HALOE trend at 20 hPa is significantly more positive than  
265 ~~the HALOE's~~ its trend at 30 hPa ( $+4.47 \pm 0.87$  %/decade), ~~although a positive difference is expected~~  
266 ~~because of the effects of the oxidation of methane to water vapor~~. Remsberg (2015, Table 1)  
267 reported significant positive trends ~~of order 10%/decade for HALOE methane~~ in the tropical

268 middle stratosphere ~~for HALOE methane of order 10%/decade~~, a small fraction (certainly less  
269 than half) of which ~~has~~ may have undergone an oxidization to SWV and a subsequent transport to  
270 40°N ~~and 20 hPa. Thus, the~~. The increase of 2.2%/decade ~~is~~ for the HALOE SWV trend from  
271 30 to 20 hPa ~~may~~ could be ~~accounted for by those processes~~ due to that process alone. Thus, it  
272 may be that the HALOE aerosol corrections ~~may be sufficiently accurate after 1992~~ at 30 hPa are  
273 reasonable over time.

274

## 275 5. Source for the springtime moistening at 40°N

276 Hegglin et al. (2014) and Remsberg (2015) showed that both methane and water vapor from  
277 limb-viewing satellite datasets (SPARC, 2017) are good indicators of seasonal variations of the  
278 BDC in the stratosphere. They reported on a hemispheric asymmetry for the net circulation,  
279 where the BDC in the northern hemisphere (NH) is stronger and its methane and relative SWV  
280 trends are more positive than in the southern hemisphere. The strength of the NH BDC is  
281 enhanced in winter, primarily due to effects of forcings from planetary waves. ~~The~~ There is  
282 chemical conversion of methane to water vapor in the middle and upper stratosphere ~~is~~ followed  
283 by descent of that relatively moist air to the lower stratosphere in the region of the polar vortex.

284

285 Seasonal SWV data from the LIMS experiment illustrate the above process for 1978-1979.  
286 Figure 8 (from Remsberg et al., 2018b, their Fig. 14) displays ~~this~~ a seasonal increase in ~~a time~~  
287 ~~series of~~ SWV ~~for~~ within the NH on the 550 K potential temperature surface (near 30 hPa) in  
288 terms of its area diagnostic versus equivalent latitude, which is a vortex-centered display of  
289 SWV along potential vorticity contours. Fig. 8 indicates that enhanced values of water vapor  
290 descended to this surface in the vortex region by early January and continued through March.  
291 Specifically, there was an equatorward expansion of the average SWV value of 5.2 ppmv to the  
292 equivalent latitude of 40°N during mid-February and from mid-March onward, as the high  
293 latitude air mixed with lower latitude air. Note that the 550 K surface is well above the tropical  
294 tropopause, minimizing effects due to any meridional exchanges of water vapor within the  
295 lowermost stratosphere. Similar analyses of seasonal changes of ozone also show that there is  
296 further descent to lower potential temperature levels during springtime and a similar transport  
297 and mixing of polar air to lower latitudes at those levels (Curbelo et al., 2021).

298

299 Polar plots of LIMS Version 6 (V6) geopotential height (GPH) and SWV for 17 February 1979  
300 are in Figures 9 and 10. They indicate the effects of meridional transport of polar air to middle  
301 latitudes, in response to a high latitude, zonal wave-2 event. Fig. 9 shows high GPH (and  
302 anticyclonic circulation) in the Aleutian and eastern Atlantic sectors and low GPH in the polar  
303 vortex (cyclonic) that extends southward across North America. The associated higher values of  
304 SWV in Fig. 10, though somewhat noisy, are characteristic of vortex air that also underwent a  
305 southward transport. The vortex (region of highest SWV) is elongated and extends equatorward  
306 around 90°E and 270°E. There is also a filament of high SWV (>5.5 ppmv) at the latitude of  
307 Boulder and across adjacent longitudes. The seasonal time series display of NH SWV in Fig. 8  
308 shows that this is when the 5.2 ppmv contour extends to near 40°N equivalent latitude.

309

310 Figure 8 also indicates that there was an initial descent of polar air with higher values of SWV to  
311 near the 31.6 hPa surface around 10 January. Then there was a more general expansion of  
312 ~~elevated SWV by the end of January~~ to the equivalent latitude of 40°N ~~by the end of January~~  
313 (follow the 4.8 ppmv contour in Fig. 8). Similar instances of meridional transport and mixing to  
314 North American middle latitudes are a likely cause of the sporadic appearance of ~~similar~~-high  
315 SWV values during the winter and early spring seasons ~~in~~of the FPH measurements ~~of~~in Fig. 43  
316 and in the recent reanalysis studies of Konopka et al. (2022) and of Wargan et al. (2023).  
317 However, the HALOE time series points in ~~Figs~~Fig. 1 ~~and 3~~ do not resolve such features ~~so well~~  
318 because they are based on averages of four or more profiles from within the rather large sector  
319 around Boulder.

320

321 HALOE SWV time series were also analyzed for occurrences of higher SWV in three separate  
322 longitude sectors (North America, 255±35°E; Aleutian, 180±35°E; and European, 35±35°E)  
323 from 1993 to 2002. There are several ~~such~~ instances at 40°N in the Boulder sector (Fig. 31), but  
324 none in the Aleutian or European sectors (not shown). ~~However~~Conversely, Figure 11 shows  
325 that there are several positive ~~SWV~~ anomalies ~~in the European sector at~~within the higher latitude  
326 zone of 53±7°N, ~~while there are in the European sector but~~ none in the Boulder or Aleutian

327 sectors (not shown). ~~Average SWV from~~ Fig. 11 ~~is 5.14 ppmv, and SWV~~ approaches 6.0  
328 ppmv in four instances (on 22 April 1994, 14 April 1996, 7 March 2000, and 14-19 February  
329 2001), ~~and average SWV is 5.14 ppmv.~~ All four instances are accompanied by low values of  
330 methane, which is ~~also~~ a tracer of the transport of polar air to lower latitudes. The instances in  
331 2000 and 2001 also occurred, ~~when just after~~ temperatures in the upper stratosphere were of  
332 order 270 K or like that for a sudden stratospheric warming (SSW) event. There was a rather  
333 extended area of higher SWV over Europe ~~at those times~~, not merely a filament of vortex air,  
334 following those events.

335

## 336 6. Summary and Conclusions

337 Analyses of time series of HALOE and FPH SWV were conducted at 30 hPa and 50 hPa for the  
338 Boulder region. Sampling frequencies for both sets of time series are ~~only~~ of the order of a  
339 week few days to a month or more several weeks. The SWV trend in the Boulder region is  
340 positive from the FPH and negative from the HALOE data from 1993 to 2005. It is assumed that  
341 the time series of FPH SWV measurements are accurate, at least or to within their uncertainties of  
342  $\pm 10\%$  to  $\pm 6\%$ ; the foregoing HALOE/FPH trend differences appear significant. However, there are  
343 rather large gaps at 40°N during late winter and spring in the HALOE time series after 2001, due  
344 to the limited power that was available for HALOE operations. This makes it is more difficult to  
345 resolve the seasonal terms and the trend term from ~~the HALOE time series data~~ after 2001.

346

347 The HALOE SWV trend goes from positive to negative around 2002, and that change is a  
348 delayed effect following the sharp decrease in tropical, lower stratospheric SWV that occurred  
349 early in 2001. The FPH time series has a trend that is less positive after 2001, too, although that  
350 change is not so obvious because of the larger scatter for its points. It is more appropriate to fit  
351 two, piecewise linear trends to both the HALOE and FPH time series with a break point in 2002.  
352 There are no known measurement biases that are affecting the HALOE trends, although,  
353 However, the retrievals of HALOE SWV do have significant and uncertain corrections for  
354 interfering aerosol extinction following the eruption of Pinatubo. ~~However, there is no clear~~  
355 evidence that those corrections are affecting, particularly at 50 hPa, where the SWV trends after

356 ~~1992. Thus, it is concluded that the from HALOE and FPH disagree. The~~ analyzed HALOE  
357 trend ~~at 30 hPa~~ (+4.47±0.87 %/decade) ~~at 30 hPa~~ agrees more closely with that from FPH  
358 (~~+5.86.9±1.2 %/decade~~) ~~for 1993 to 2002 within their combined uncertainties~~, or where the  
359 aerosol corrections are relatively small after 1992.

360  
361 The HALOE SWV time series at 20 hPa clearly shows a springtime maximum. Northern  
362 hemisphere SWV time series from the Limb Infrared Monitor of the Stratosphere (LIMS)  
363 experiment indicate a transport of higher SWV from polar to middle latitudes during late winter  
364 and springtime. Daily surface maps of LIMS SWV reveal ~~instances of~~ filamentary structure at  
365 the latitude of 40°N during and following dynamically active periods. Surface maps of GPH  
366 verify that there was meridional transport of high SWV from the polar vortex to the latitude of  
367 40°N at those times. Whereas FPH measurements sense SWV variations at all scales, the  
368 HALOE time series ~~of the present study~~ do not resolve intermediate to smaller scale structure  
369 because its data points are based on an average of four or more occultation profiles within a  
370 finite latitude/longitude sector centered on Boulder. It is concluded that the variations and trends  
371 of HALOE SWV are reasonably accurate at 40°N and 30 hPa for 1993 to 2002 and in accord  
372 with the spatial scales of its measurements and its sampling frequencies.

373

#### 374 **Data Availability**

375 The LIMS V6 Level 3 product and the HALOE V19 profiles are at the NASA EARTHDATA  
376 site of EOSDIS and its Website as:

377 [https://disc.gsfc.nasa.gov/datacollection/LIMSN7L3\\_006.html](https://disc.gsfc.nasa.gov/datacollection/LIMSN7L3_006.html), and as

378 [https://disc.gsfc.nasa.gov/datacollection/UARHA2FN\\_019.html](https://disc.gsfc.nasa.gov/datacollection/UARHA2FN_019.html), respectively.

379 Frost point hygrometer (Lev) data were downloaded from the NOAA website:

380 [https://gml.noaa.gov/aftp/data/ozwv/WaterVapor/Boulder\\_New/](https://gml.noaa.gov/aftp/data/ozwv/WaterVapor/Boulder_New/).

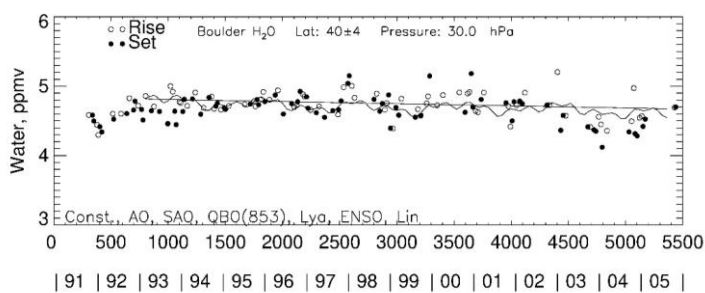
381

382 *Competing interests:* The author declares no competing interests.

383

384 *Acknowledgements.* Author EER thanks V. Lynn Harvey for generating the plot in Figure 8 that  
385 appeared originally in Remsberg et al. (2018b). EER also appreciates comments by Mark Hervig  
386 about on a draft of the manuscript. EER carried out this work while serving as a Distinguished  
387 Research Associate of the Science Directorate at NASA Langley.

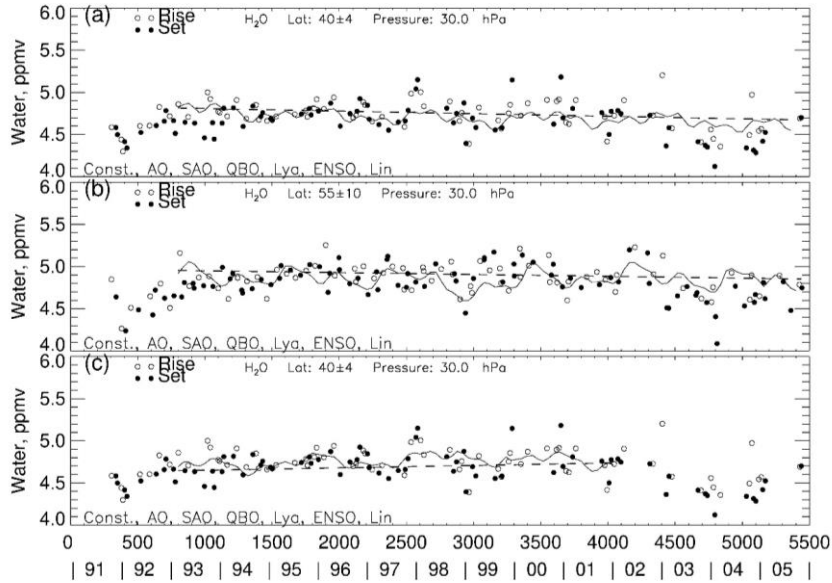
388  
389



390  
391

Formatted: Space After: 8 pt, Line spacing: Multiple  
1.08 li

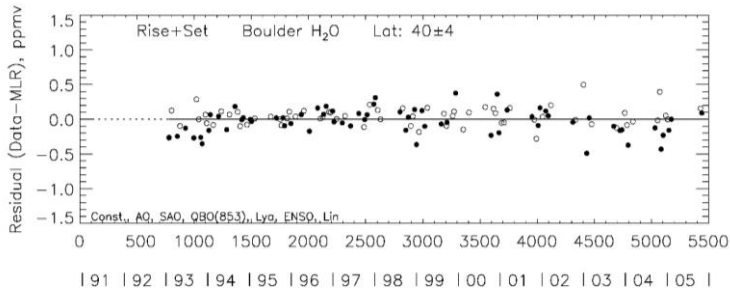
392



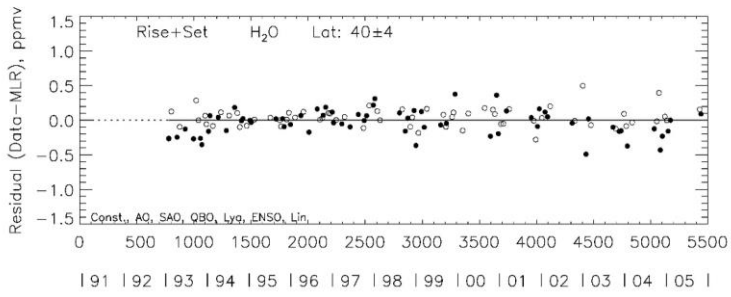
393

394 Figure 1—MLR fit to a HALOE SWV time series ~~for the region above;~~ (a) Boulder sector,   
 395 40°N, 1993-2005, (b) at 55°N, and (c) 40°N, 1993-2002. The fit of all the MLR terms is ~~shown~~   
 396 as the oscillating curve; the linear trend term is the straight dashed line. Time ~~{by year or in~~   
 397 days) ~~and year~~ on abscissa begins on ~~January Jan.~~ 1, 1991.

398



399



400

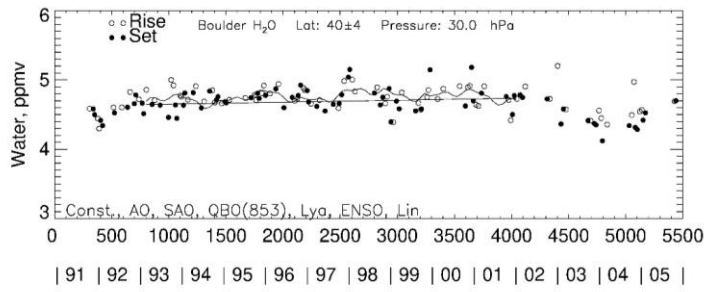
401 Figure 2—Residual from MLR model fit to HALOE time series data of Fig. 1-(a).

402

403

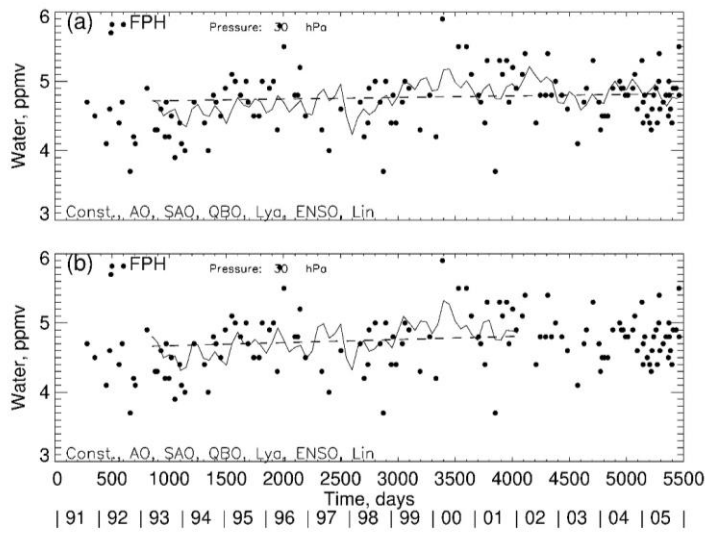
404

Formatted: Line spacing: 1.5 lines



405

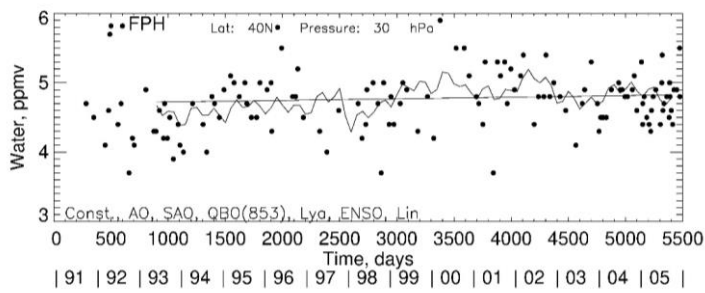




406

407 Figure 3—As in Fig. 1, but where the MLR fit for 40°N is from 1993 to 2002.

408



409

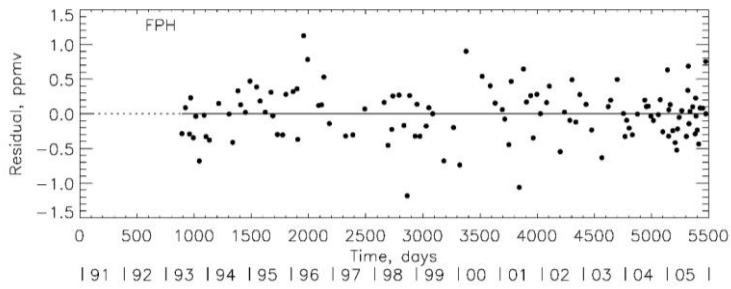
410 Figure 4—Time series of FPH data and MLR fit to them for comparison with Fig. 41; (a) 1993-  
411 2005, (b) 1993-2002.

412

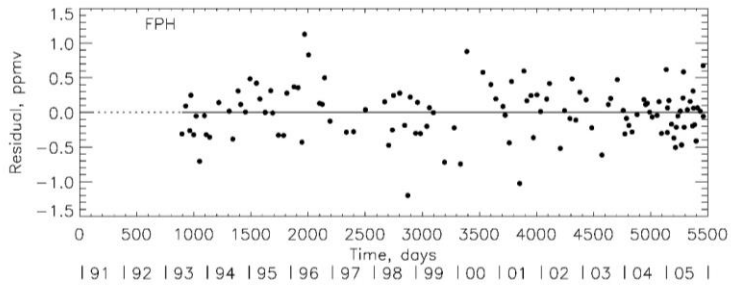
413

414

415  
416  
417  
418



419



420

---

421 Figure 54—Time series residual for the MLR fit to the FPH data of Fig. 4-3(a).

422

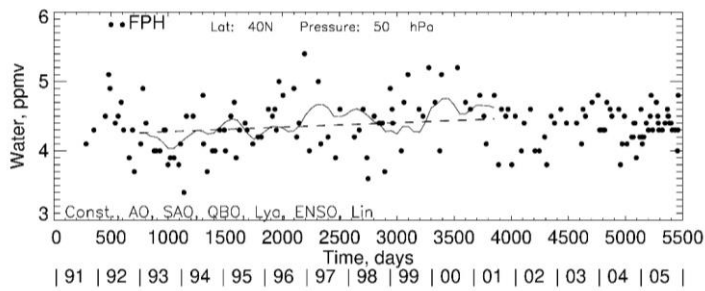
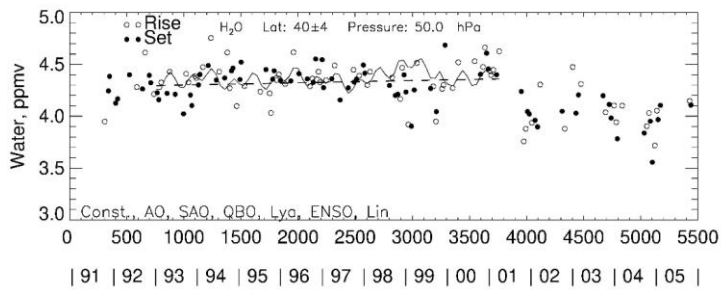
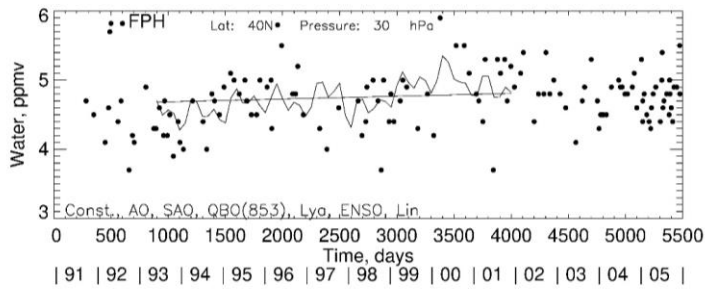
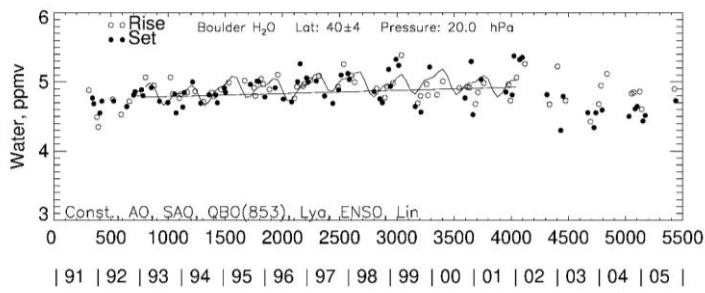


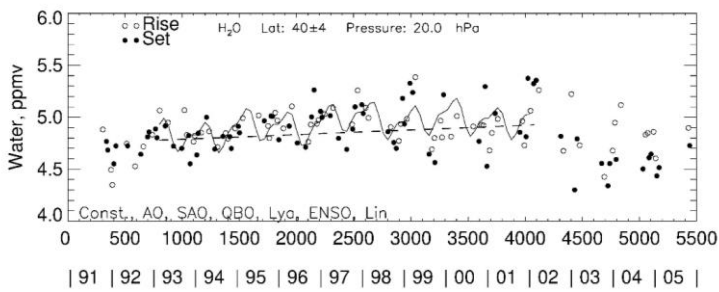
Figure 5—HALOE time series data at 50 hPa and MLR fit to them for 1993 to 2002.

Figure 6—As in Fig. 45, but for 1993 to 2002 FPH data.

431  
432  
433  
434  
435  
436  
437  
438  
439  
440



441  
442

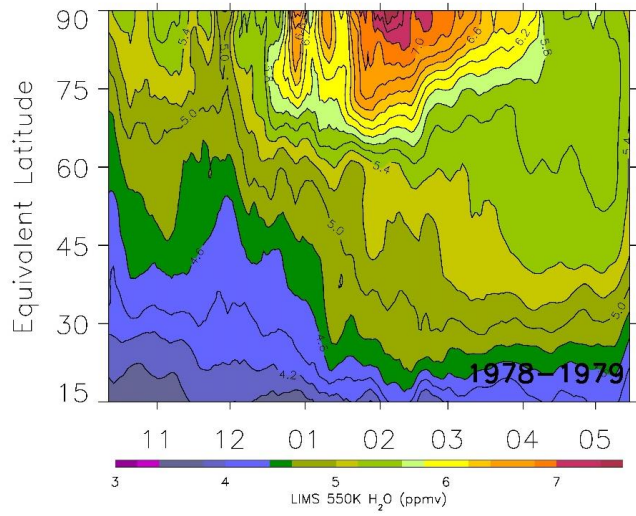


443

444 Figure 7—As in Fig. 3, but for HALOE time series data at 20 hPa and MLR fit to them for 1993  
445 to 2002.

Formatted: Font: +Body (Calibri), 11 pt

446

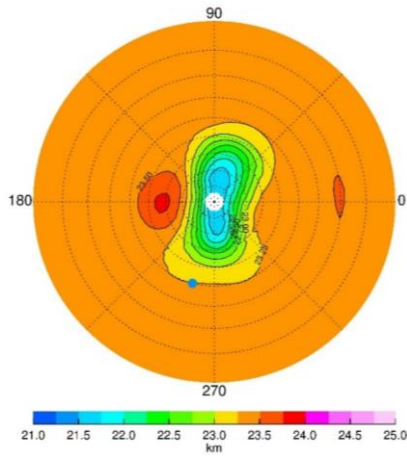


447

448 Figure 8—Time series of LIMS water vapor vs. equivalent latitude at 550 K and with smoothing  
449 over 7 days. Contour interval is 0.2 ppmv. Tic marks along the abscissa denote the middle of  
450 each month.

451

452



453

454 Figure 9—NH plot on the 31.6-hPa surface for 17 February 1979 of LIMS geopotential height  
 455 (GPH). Contour increment for GPH is 0.25 gpm, and dashed circles are at every 10° of  
 456 latitude. Blue dot is location of Boulder, CO (40°N, 255°E).

457

458

459

460

461

462

463

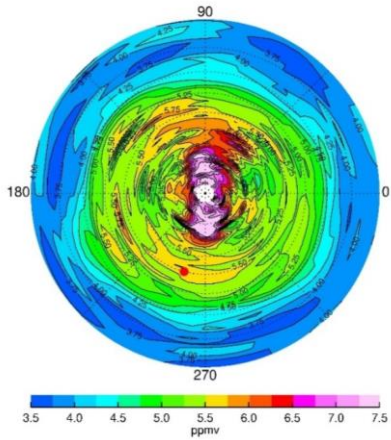
464

465

466

467

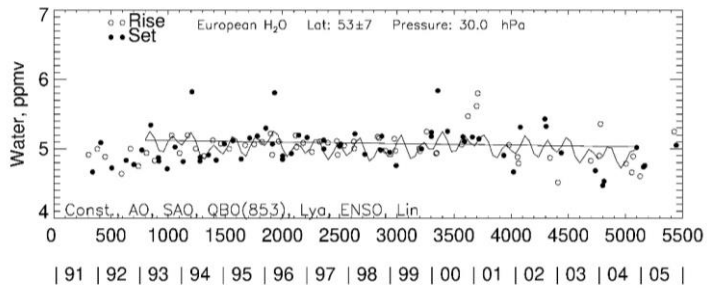
468



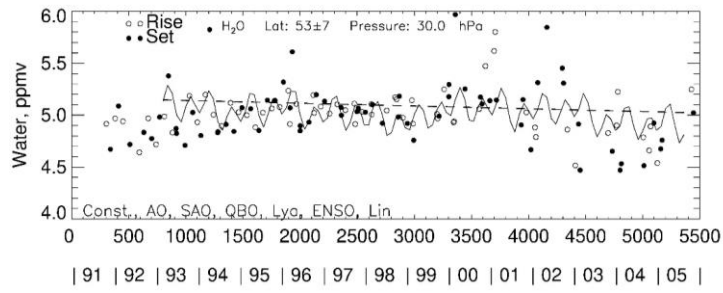
469

470 Figure 10—As in Fig. 9, but for LIMS SWV on 17 February. Contour interval (CI) is 0.25  
 471 ppmv. Red dot is location of Boulder.

472



473



474

475 Figure 11—As in Fig. 1-(a), but for a European sector, centered at 53°N, 35°E. **Note that the**  
 476 **HALOE SWV scale extends from 4 to 7 ppmv, unlike in Fig. 1.**

477

478

479

480



481 **References**

482 [Bhatt, P. P., Remsberg, E. E., Gordley, L. L., McInerney, J. M., Brackett, V. G., and Russell III,](#)  
483 [J. M.: An evaluation of the quality of Halogen Occultation Experiment ozone profiles in the](#)  
484 [lower stratosphere, J. Geophys. Res., 104, <https://doi.org/10.1029/1999JD900058>, 1999.](#)

485  
486 [Charlton, A. J., and Polvani, L. M.: A New Look at Stratospheric Sudden Warmings. Part I:](#)  
487 [Climatology and Modeling Benchmarks, J. Climate, 20, <https://doi.org/10.1175/JCLI3996.1>,](#)  
488 [2007.](#)

489  
490 Curbelo, J., Chen, G., & Mechoso, C. R.: Lagrangian analysis of the northern stratospheric polar  
491 vortex split in April 2020. Geophys. Res. Lett., 48, e2021GL093874.  
492 <https://doi.org/10.1029/2021GL093874>, 2021.

493  
494 Davis, S. M., Rosenlof, K. H., Hassler, B., Hurst, D. F., Read, W. G., Vömel, H., Selkirk, H.,  
495 Fujiwara, M., and Damadeo, R.: The stratospheric water and ozone satellite homogenized  
496 (SWOOSH) database: a long-term database for climate studies, Earth Syst. Sci. Data, 8, 461-490,  
497 [www.earth-syst-sci-data.net/8/461/2016/doi:10.5194/essd-8-461-2016](http://www.earth-syst-sci-data.net/8/461/2016/doi:10.5194/essd-8-461-2016), 2016.

498  
499 Gordley, L. L., Thompson, E., McHugh, M., Remsberg, E., Russell III, J., and Magill, B.:  
500 Accuracy of atmospheric trends inferred from the Halogen Occultation Experiment data, J. Appl.  
501 Remote Sensing, 3, <https://doi.org/10.1117/1.3131722>, 2009.

502  
503 [Hall, E. G., Jordan, A. F., Hurst, D. F., Oltmans, S. J., Vömel, H., Kühnreich, B., and Ebert, V.:](#)  
504 [Advancements, measurement uncertainties, and recent comparisons of the NOAA frost point](#)  
505 [hygrometer, Atmos. Meas. Tech., 9, <https://doi.org/10.5194/amt-9-4295-2016>, 2016.](#)

506  
507 Harries, J. E., Russell III, J. M., Tuck, A. F., Gordley, L. L., Purcell, P., Stone, K., Bevilacqua,  
508 R. M., Gunson, M., Nedoluha, G., and Traub, W. A.: Validation of measurements of water vapor

Formatted: Font: Not Bold  
Formatted: Space After: 6 pt, Line spacing: 1.5 lines

509 from the Halogen Occultation Experiment (HALOE), J. Geophys. Res., 101,  
510 <https://doi.org/10.1029/95JD02933C>, 1996.

511

512 Hegglin, M. I., Plummer, D. A., Shepherd, T. G., Scinocca, J. F., Anderson, J., Froidevaux, L.,  
513 Funke, B., Hurst, D., Rozanov, A., Urban, J., von Clarmann, T., Walker, K. A., Wang, H. J.,  
514 Tegtmeier, S., and Weigel, K.: Vertical structure of stratospheric water vapour trends derived  
515 from merged satellite data, Nature Geoscience, 7(10), 768–776.  
516 <https://doi.org/10.1038/NGEO2236>, 2014.

517

518 Hervig, M. E., Russell III, J. M., Gordley, L. L., Park, J. H., Drayson, S. R., and Deshler, T.:  
519 Validation of aerosol measurements from the Halogen Occultation Experiment, J. Geophys. Res.,  
520 101, <https://doi.org/10.1029/95JD02464>, 1996.

521

522 Hervig, M. E., Russell III, J. M., Gordley, L. L., Daniels, J., Drayson, S. R., Park, J. H.: Aerosol  
523 effects and corrections in the Halogen Occultation Experiment, J. Geophys. Res., 100,  
524 <https://doi.org/10.1029/94JD02143>, 1995.

525

526 Hurst, D. F., ~~Fujiwara, M., and Oltmans, S.:~~ Frost point hygrometers, in *Field Measurements for*  
527 *Passive Environmental Remote Sensing*, Elsevier, Inc., [https://doi.org/10.1016/B978-0-12-](https://doi.org/10.1016/B978-0-12-823953-7.00015-0)  
528 [823953-7.00015-0](https://doi.org/10.1016/B978-0-12-823953-7.00015-0), 2023.

529

530 ~~Hurst, D. F.,~~ Oltmans, S. J., Vömel, H., Rosenlof, K. H., Davis, S. M., Ray, E. A., Hall, E. G.,  
531 and Jordan, A. F.: Stratospheric water vapor trends over Boulder, Colorado: Analysis of the 30  
532 year Boulder record, J. Geophys. Res., 116, <https://doi.org/10.1029/2010JD015065>, 2011.

533

534 Konopka, P., Tao, M., Ploeger, F., Hurst, D. F., Santee, M. L., Wright, J. S., and Riese, M.:  
535 Stratospheric moistening after 2000, Geophysical Research Letters, 49, e2021GL097609.  
536 <https://doi.org/10.1029/2021GL097609>, 2022.

537

538 Lossow, S., Hurst, D. F., Rosenlof, K. H., Stiller, G. P., von Clarmann, T., Brinkop, S., Dameris,  
539 M., Jöckel, P., Kinnison, D. E., Plieninger, J., Plummer, D. A., Ploeger, F., Read, W. G.,  
540 Remsberg, E. E., Russell III, J. M., and Tao, M.: Trend differences in lower stratospheric water  
541 vapour between Boulder and the zonal mean and their role in understanding fundamental  
542 observational discrepancies, *Atmos. Chem. Phys.*, 18, 8331-8351, [https://doi.org/10.5194/acp-](https://doi.org/10.5194/acp-18-8331-2018)  
543 [18-8331-2018](https://doi.org/10.5194/acp-18-8331-2018), 2018.

544

545 Manney, G. L., Millan, L. F., Santee, M. L., Wargan, K., Lambert, A., Neu, J. L., Werner, F.,  
546 Lawrence, Z. D., Schwartz, M. J., Livesey, N. J., and Read, W. G.: Signatures of Anomalous  
547 Transport in the 2019/2020 Arctic Stratospheric Polar Vortex, *J. Geophys. Res. Atmospheres*,  
548 127, e2022JD037407, <https://doi.org/10.1029/2022JD037407>, 2022.

549

550 [Randel, W. J., Wu, F., Vömel, H., Nedoluha, G. E., and Forster, P.: Decreases in stratospheric](#)  
551 [water vapor after 2001: Links to changes in the tropical tropopause and the Brewer-Dobson](#)  
552 [circulation, \*J. Geophys. Res. Atmospheres\*, 111, <https://doi.org/10.1029/2005JD006744>, 2006.](#)

553

554 Remsberg, E.: Methane as a diagnostic tracer of changes in the Brewer-Dobson circulation of the  
555 stratosphere, *Atmos. Chem. Phys.*, 15, 3739-3754, <https://doi.org/10.5194/acp-15-3739-2015>,  
556 2015.

557

558 Remsberg, E. E.: On the response of Halogen Occultation Experiment (HALOE) stratospheric  
559 ozone and temperature to the 11-yr solar cycle forcing, *J. Geophys. Res.-Atmospheres*, 113,  
560 <https://doi.org/10.1029/2008JD010189>, 2008.

561

562 Remsberg, E., Damadeo, R., Natarajan, M., and Bhatt, P.: Observed responses of mesospheric  
563 water vapor to solar cycle and dynamical forcings, *J. Geophys. Res.*, 123, 3830-3843,  
564 <https://doi.org/10.1002/2017JD028029>, 2018a.

565

566 Remsberg, E., Natarajan, M., and Harvey, V. L.: On the consistency of HNO<sub>3</sub> and NO<sub>2</sub> in the  
567 Aleutian High region from the Nimbus 7 LIMS Version 6 dataset, *Atmos. Meas. Tech.*, 11,  
568 3611-3626, <https://doi.org/10.5194/amt-11-3611-2018>, 2018b.

569

570 Scherer, M., Vömel, H., Fueglistaler, S., Oltmans, S.J., and Staehelin, J.: Trends and variability  
571 of midlatitude stratospheric water vapour deduced from the re-evaluated Boulder balloon series  
572 and HALOE, *Atmos. Chem. Phys.*, 8, 1391–1402, [www.atmos-chem-phys.net/8/1391/2008/](http://www.atmos-chem-phys.net/8/1391/2008/),  
573 2008.

574

575 ~~SPARC Report No. 2: Upper Tropospheric and Stratospheric Water Vapour, Edited by D. Kley,  
576 J. M. Russell III, and C. Phillips, WCRP—113, Geneva, [https://www.sparc-  
578 climate.org/publications/sparc-reports/sparc-report-no-2/](https://www.sparc-<br/>577 climate.org/publications/sparc-reports/sparc-report-no-2/), 2000.~~

579 ~~SPARC Report No. 8 of the SPARC Data Initiative: Assessment of stratospheric trace gas and  
580 aerosol climatologies from satellite limb sounders, Prepared by the SPARC Data Initiative Team  
581 and edited by M. I. Hegglin and S. Tegtmeier, WCRP-5/2017, Geneva,  
582 <https://doi.org/10.3929/ethz-a-010863911>, 2017.~~

583

584 ~~Tiao, G. C., Reinsel, G. C., Xu, D., Pedrick, J. H., Zhu, X., Miller, A. J., DeLuisi, J. J., Mateer,  
585 C. L., and Wuebbles, D. J.: Effects of autocorrelation and temporal sampling schemes on  
586 estimates of trend and spatial correlation, *J. Geophys. Res.*, 95, 20507–20517,  
587 <https://doi.org/10.1029/JD095iD12p20507>, 1990.~~

588

589 Wargan, K., Weir, B., Manney, G. L., Cohn, S. E., Knowland, K. E., Wales, P. A., and Livesey,  
590 N. J.: M2-SCREAM: A stratospheric composition reanalysis of Aura MLS data with MERRA-2  
591 transport. *Earth and Space Science*, 10, e2022EA002632.,  
592 <https://doi.org/10.1029/2022EA002632>, 2023.

